Perinatal Reduction of Genetically Aberrant Neurons from Human Cerebral Cortex

Authors: Diane D. Shao[1,2,†], MD, PhD, Yifan Zhao[3,4,†], BS, Urmi Ghosh[2,5], BA, Joseph Brew[3], Sijing Zhao[2,6], Xuyu Qian[2,5], Julie Tran[3], Takumi Taketomi[7], Fuminori Tsuruta[7,8], PhD, Peter J. Park, PhD[3,†,*], Christopher A. Walsh, MD, PhD[1,2,5,†,*]

Affiliations:

1. Department of Neurology, Boston Children's Hospital, Boston, MA
2. Department of Pediatrics, Division of Genetics and Genomics, Boston Children's Hospital, Boston, MA
3. Department of Biomedical Informatics, Harvard Medical School, Boston, MA
4. Program in Health Sciences & Technology, Harvard Medical School & Massachusetts Institute of Technology, Boston, MA, USA
5. Howard Hughes Medical Institute, Chevy Chase, MD
6. Biological and Biomedical Sciences Graduate Program, Harvard Medical School, Boston, MA
7. Ph.D. Program in Human Biology, University of Tsukuba, Tsukuba, Ibaraki, Japan
8. Institute of Life and Environmental Sciences, University of Tsukuba, Tsukuba, Ibaraki, Japan

† These authors contributed equally to this work.

* Correspondence: Christopher.Walsh@childrens.harvard.edu; Peter_park@hms.harvard.edu

Abstract

Since human neurons are postmitotic and long-lived, the regulation of their genomic content is crucial. Normal neuronal function is uniquely dependent on gene dosage, with diverse genome copy number alterations (CNA) associated with neurodevelopmental and neuropsychiatric conditions[1–3]. In this study, we evaluated the landscape of CNA arising in normal human brains, focusing on prenatal and perinatal ages. We surveyed ~5,897 CNA in >1,200 single neurons from human postmortem brain of individuals without a neurological diagnosis, ranging in age from gestational week (GW) 14 to 90 years old. Using Tn5-based single-cell whole-genome amplification (scWGA) and informatic advances to validate CNAs in single neurons, we determined that a striking proportion of neurons (up to 45%) in human prenatal cortex showed aberrant genomes, characterized by large-scale CNAs in multiple chromosomes, which reduces significantly during the perinatal period ($p<0.1$). Furthermore, we identified micronuclei in the developing cortex, reflecting genetic instability reminiscent of that described in early embryonic development[4–6]. The scale of CNA appeared to alter the trajectory of neuronal elimination, as subchromosomal CNAs were more slowly eliminated, over the course of a lifetime. CNAs were depleted for dosage-sensitive genes and genes involved in neurodevelopmental disorders ($p<.05$), and thus represent genomic quality control mechanisms that eliminate selectively those neurons with CNA involving critical genes. Perinatal elimination

of defective neuronal genomes may in turn reflect a developmental landmark essential for normal cognitive function.

Main Text

Genome-scale copy number alterations (CNA) are increasingly recognized as common in early human development, with up to 73% of embryos exhibiting large chromosomal aberrations in the early post-zygotic phase[4,7–9]. Analogously, in human neuronal progenitors, extensive mosaic aneuploidy involving at least 10-30% of progenitors have been reported[10,11]. In contrast, the mature human brain is exquisitely sensitive to gene copy number. Autism, schizophrenia, epilepsy, intellectual disability and other neuropsychiatric conditions are all commonly caused by chromosomal or sub-chromosomal CNA, as well as by heterozygous loss of function (LoF) mutations in more than one thousand essential genes[12–14]. Genes involved in these conditions often encode structural proteins of the synapse, or regulators of synaptic plasticity, suggesting that key aspects of neuronal plasticity underlying these conditions are intensely sensitive to gene dosage[15,16].

Despite the aneuploidy reported in neuronal progenitors, analyses of neurons from adult postmortem human brain reveal much more modest, predominantly sub-chromosomal CNAs[17–19]. One hypothesis is that neuronal progenitors are cycling cells that undergo genome quality control mechanisms classically related to cell cycle regulation that prevents the establishment of neurons carrying these CNA. An alternative, previously unexplored, hypothesis is that genetically aberrant neurons establish themselves in the cerebral cortex and that selective forces act on post-mitotic neurons. While numerous mechanisms have been described in developing brain that ultimately create an appropriate postnatal collection of neurons, including morphogenetic and programmed cell death[20], synaptic pruning[21], and autophagy[22], the impact of genotype as a component that determines the final neuronal population has never been addressed. Using single-cell whole genome sequencing, we describe large-scale genetic copy number aberrations during brain expansion, analogous to aberrations observed in early post-zygotic fertilization. These data highlight a paradox of how postmitotic neurons, which lack the genome quality control mechanisms available to cycling cells, resolve large-scale genomic events during development, and provides a paradigm for genetic control in postmitotic cells of the developing human brain.

Accurate copy number detection in single prenatal neurons

In order to directly evaluate the landscape of structural variation in the human prenatal brain, we generated single-cell whole genome sequencing (scWGS) from 1,298 neurons and developed a novel informatic tool for validating CNA. We generated data from postmortem, non-diseased brains from seven human prenatal donors ranging from GW 14-25, and nine postnatal brains from infancy through age 90 years (Fig. 1a, S1). To obtain a pure population of postmitotic cerebral cortical neurons, we cryodissected the human prenatal cortical plate, which can be visualized in a dissecting microscope (Fig 1b). Dissection of cortical plate neurons provides a population that is essentially exclusively postmitotic, noncycling neurons, since neuronal

progenitor cells (NPCs) and glial nuclei are located in deeper cortical regions. Neurons migrate into the cortical plate after withdrawing from the cell cycle and becoming permanently postmitotic. We confirmed using single-cell RNA sequencing (scRNAseq) that our cortical plate dissection yielded 98% purity for neurons (Fig. 1b, S1b). Diploid neuronal nuclei were sorted into microwells based on DAPI content, and single-cell whole genome libraries were generated using Tn5-based amplification (TbA) and sequenced at ~0.05X coverage. Because the quality of sequencing libraries may affect downstream variant detection, we confirmed that all samples were of high uniformity (low MAPD[23] score) and read-count (Fig. S1d-e). We additionally used principal component analysis to cluster neurons based on coverage patterns across the genome to remove poor quality cells (Fig. S2).

We greatly improved calling methods for genome-wide CNA accurately from TbA by developing an orthogonal approach to validate copy number calls. To accurately detect CNA, we first applied our recently developed CNA caller (HiScanner[24]), and subsequently applied a new validation metric, Fragment Overlap Density (FOD). FOD is determined by evaluating the overlap density of aligned molecules, which will be different based on the total number of alleles present when Tn5-based approaches are applied in single cells (Fig. 1c). FOD is less affected by amplification biases in scWGS compared to traditional read-depth-based CNA calling approaches and improves detection in real and simulated CNA scenarios (Fig. S3). Importantly, fragment overlap patterns can provide additional information for CNA inference where the read-depth signal is ambiguous. For example, in a copy loss region where only one homolog is present, no fragment overlaps should be observed. We apply the FOD metric to reject individual copy loss and copy gains from HiScanner that are not supported by the FOD metric (Fig. 1d). We find that while FOD validation affects some CNA calls in the majority of cells, a subpopulation of high-quality cells undergoes frequent correction after FOD validation (Fig. 1e). Because single-cell whole genome amplification (scWGA) destroys the original cellular substrate in the process of amplification, this approach represents an advance over prior methods that are unable to validate detected CNAs in postmitotic cells.

Our increased confidence in CNA calling enabled us to identify a subset of postmitotic neurons in the prenatal cortical plate that had genome-wide aberrant patterns of copy number gains and losses on multiple chromosomes. Gains or losses could be present within the same chromosome, even after FOD validation. Numerous chromosomes may be affected at loci across the genome, suggesting a genome-wide process (Fig. 1f).

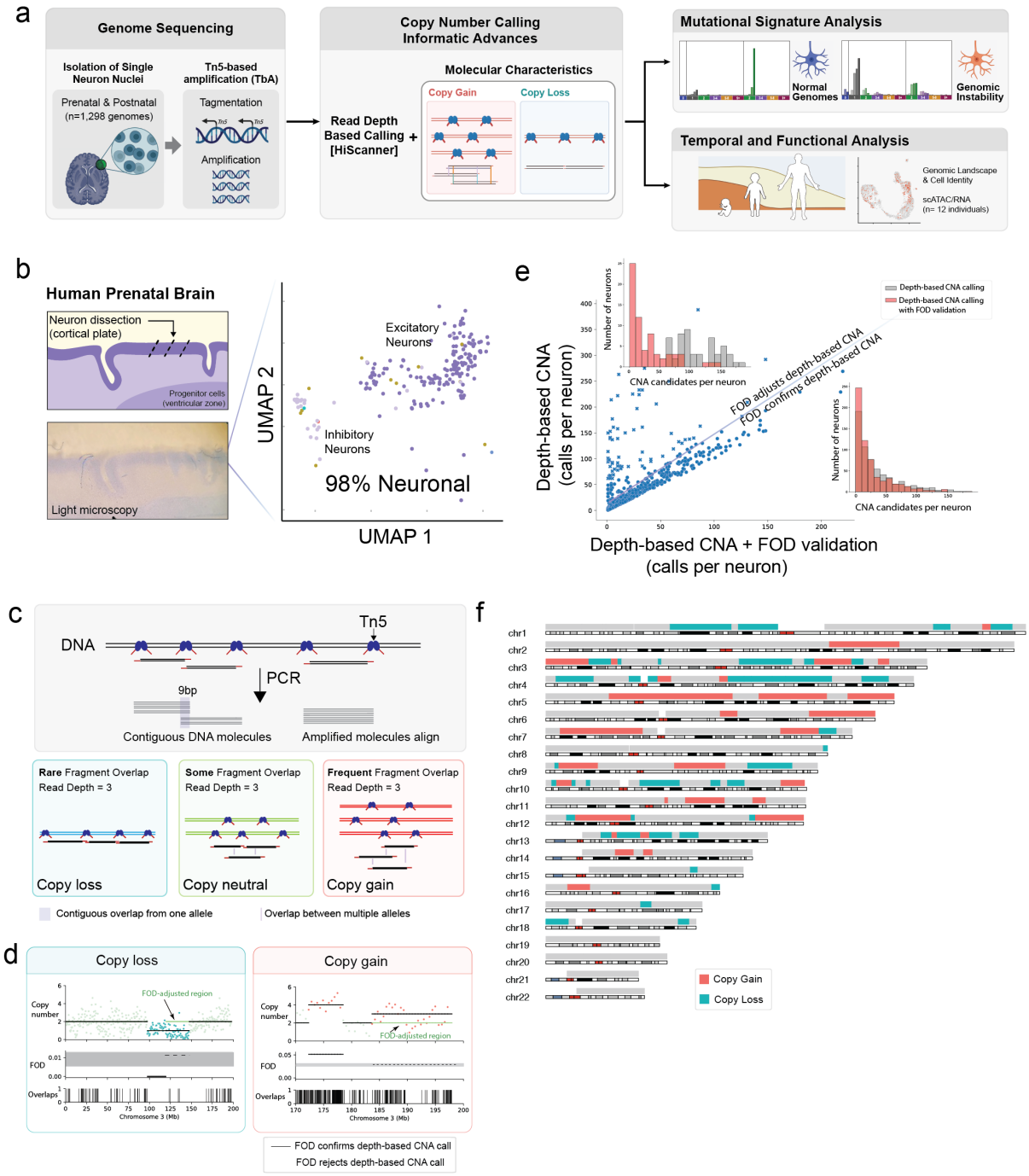

Figure 1. Single human fetal neurons identified with genome-wide aberrant copy number patterns.

A. Overview of study design and data analyzed.
B. Single-cell RNA sequencing confirms neuronal nuclei were obtained from cortical plate dissection of normal prenatal human brain. Neuronal nuclei (dark and light purple); non-neuronal nuclei (other shades).
C. Schematic illustration of Tn5-based amplification libraries in which single-genomes create distinct patterns of molecular overlap that distinguishes copy number states.

D. Example gains and losses from a single cell, indicating usage of the molecular overlap metric (Fragment Overlap Density) to validate depth-based single-cell copy number calls. CNA calls adjusted after FOD validation (green). Grey band in FOD track indicates the 95% confidence interval of FOD in diploid regions of the cell.
E. Distribution of CNA calls per cell before and after FOD validation. Histograms demonstrate that FOD creates a large impact on CNA calls for many neurons.
F. Representative single prenatal human cortical neuron that exhibits widespread CNA across multiple chromosomes.

Evidence of neuronal genomic instability

Prenatal neurons from the cerebral cortex exhibited striking patterns of gains and losses genome-wide in a subset of neurons (Fig. 2a). Copy losses were more frequent than copy gains, with 68.2% (2523/3698) of CNA in prenatal samples being copy losses, and 31.8% (1175/3698) copy gains (Fig. 2b). We defined aneuploidy as a chromosome whose total losses or gains involved at least half the chromosome. Interestingly, while most aneuploid cells had only one aneuploid chromosome, some cells displayed aneuploidy on multiple chromosomes (Fig. 2c).

Since genomic instability during zygotic cell divisions and in cancer are associated with micronuclei, which encapsulate otherwise aberrantly positioned DNA[4,25,26], we hypothesized that micronuclei would be present in prenatal neurons. First, we performed high-resolution microscopy on fixed slices of human fetal brain at mid-gestation stained with DAPI, and identified micronuclei structures in multiple samples (Fig. 2d). We confirmed that these micronuclei structures were neuronal in content by immunostaining micronuclei with the neuronal marker, SATB2 (Fig. 2e). Micronuclei were seen to be associated with ~6% of primary nuclei (Table S1). Micronuclei were also present in the ventricular zone, which is populated by NPCs, but were further increased in frequency among the postmitotic neurons of the cortical plate. The first reports of micronuclei in the neuronal cortex were observed in murine cells[27], and intriguingly showed that the fragmentation of the genome and formation of micronuclei occurred both in the ventricular zone and additionally during the migration of neurons into the cortical plate. Our data concordantly shows the increased presence of micronuclei in the cortical plate (Table S2), suggesting that mechanisms of genetic instability operate at the level of neuronal migration and maturation.

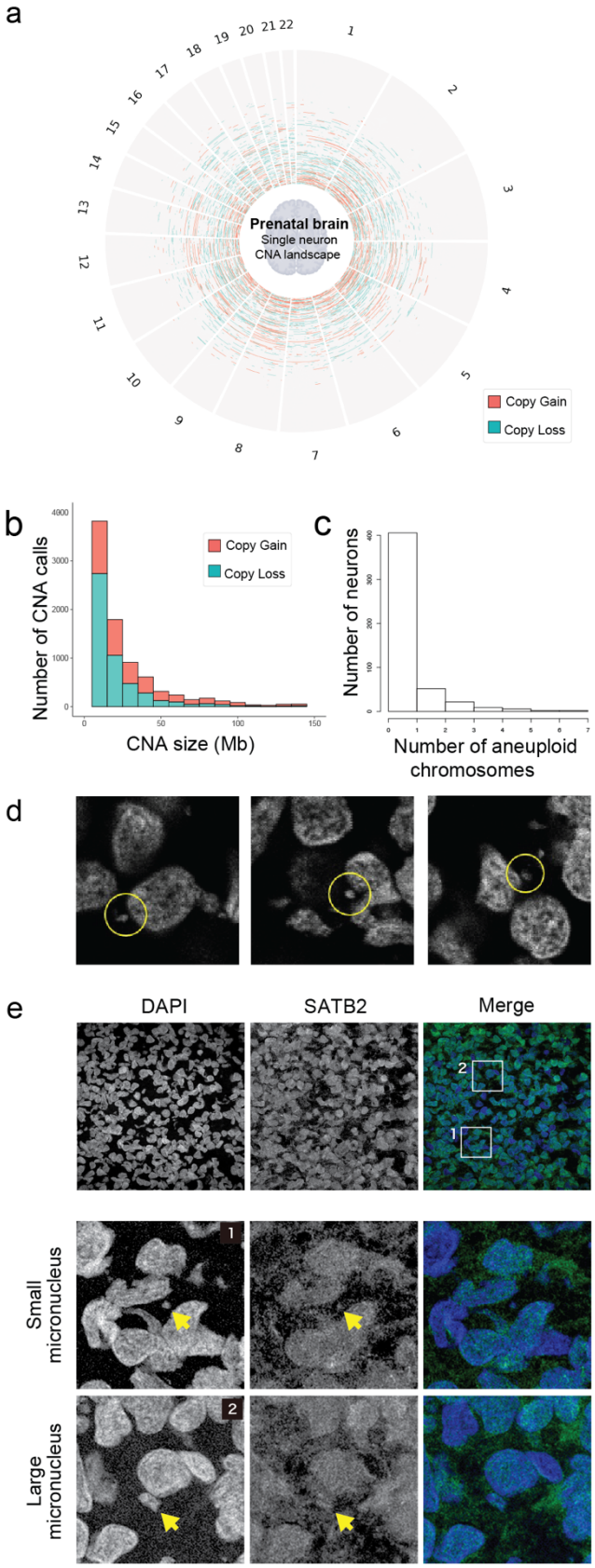

Figure 2. Genome-scale genetic events in prenatal postmitotic neurons are associated with genetic instability.

A. Circos plot of gains and losses across all chromosomes in human prenatal neurons. Red represents copy gains and blue represents copy losses.
B. Distribution of sizes of copy gains or losses in prenatal neurons.
C. Distribution of number of aneuploid chromosomes in each cell. A chromosome was defined as aneuploid if copy number alterations were more than half of the total chromosome size.
D. Micronuclei, signs of genetic instability, are present in the human cortical plate of the human prenatal brain.
E. Micronuclei in the cortical plate are observed in neuronal nuclei, marked by SATB2 staining.

Copy number signatures classify aberrant genomes with large-scale CNA

In order to interpret the diverse CNA patterns in the neurons, we classified our data to fit copy number signatures generated through analysis of the Cancer Genome Atlas COSMIC data[28]. Each signature describes a specific pattern of copy number states as well as copy number size. We categorized CNA profiles into distinct "signature" groups. Adapting the concept of mutational signature analysis[28], our aim was to reduce the dimensionality of CNA profiles—including types, sizes, and locations—and identify common patterns, an approach previously validated for CNA analysis in cancer. We determined that copy number profiles in neurons most closely resembled combinations of four COSMIC CNA signatures that we named based on their key characteristics: CN1: Diploid Predominant, CN1+CN2: Gain Predominant, CN1+CN9: Focal Loss Predominant, and CN1+CN13: Broad Loss Predominant (Fig. 3a-c, S4). Mean cosine similarities of our neuronal signatures in each category to COSMIC signature patterns were 0.98, 0.98, 0.92, and 0.96, respectively. Each cell was comprised of combinations of these signatures (Fig. 3b-c). We refer to the three categories of Gain, Focal, and Broad Loss Predominant as patterns of "large-scale CNA", highlighting their characteristic involvement of multiple chromosomes throughout the genome. The Diploid Predominant cluster contained cells with CN1 signature alone, and were diploid with a subset of cells harboring sub-chromosomal CNA. The resemblance of neuronal CNA signatures to those defined in COSMIC suggest that they likely occur in dividing cells, presumably early embryonic and later neural progenitor cells.

In postnatal samples, the proportion of neurons with large-scale CNAs decreased significantly ($p=0.0082$; Student's t-test, two tailed) (Fig. 3d, S5). Specifically, focal and broad loss-predominant cells decreased by more than 50%, while the proportion of diploid-predominant cells increased correspondingly. The number of CNA per cell also decreased between prenatal and postnatal samples, and the same was true within each signature category (Fig. S4).

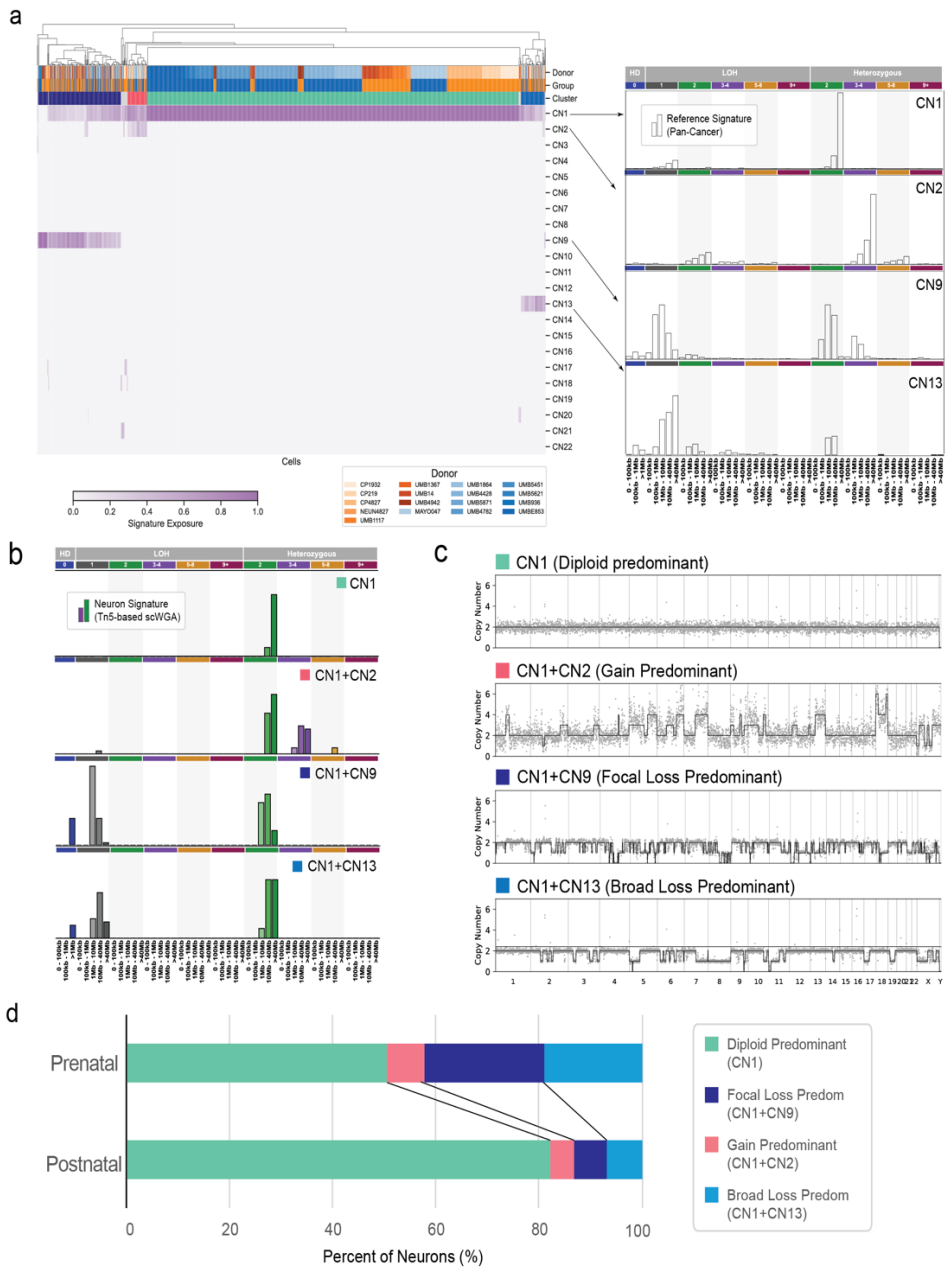

Figure 3. Large-scale genomic events are associated with copy number mutational signatures.

A. Single-neuron copy number profile signature decomposition. Signature IDs with prefix "CN" refer to those described in COSMIC catalog[28]. Clusters are defined by hierarchical clustering.
B. Copy number signatures represented by the four primary signature clusters identified across all human neurons.
C. Representative single-cell copy number profiles of each of the four clusters.
D. Proportion of neurons in each signature category observed in human prenatal and postnatal neurons.

Due to the surprisingly high proportion of cells that we identified with large-scale CNA, we evaluated whether disruption of nuclear integrity may falsely elevate our CNA rates. We used TbA to generate single-cell CNA mutational signatures in an NPC line for which we disrupted nuclear integrity by applying 24 hours of staurosporin treatment (Fig. S6). Indeed, we found many cells with disrupted nuclear integrity failed to pass quality control and were excluded; however the passing cells had large-scale CNV rate of only 9% (three of 33 cells). We thus concluded that our false discovery rate for large-scale CNA cells is conservatively 9% (Fig. S6b-c). However, as we might expect NPC in culture to be subject to some of the same genetic forces as the human brain, these abnormalities may represent true genetic changes. Notably the same 4 subgroups were seen in the NPC mutational signature decomposition as that of the human brain (Fig. S6c).

We hypothesized that if cells with large-scale CNA are indeed being cleared from the brain over time, we would see a corresponding clearance of micronuclei that arose related to early genetic instability. To test this hypothesis, we isolated micronuclei by serial gradient sucrose fractionation with visualization to identify micronuclei enriched content as previously described[29]. We sequenced the micronuclei fraction and nuclei fraction for brains at prenatal, infancy, and elderly ages and compared this to the genetic content in the nuclear fraction in the same sample (Fig. S7; Table S3). We found that the that the genetic content of micronuclei fractions deviated strikingly from the genetic content of nuclei fractions in the prenatal brains, and that this difference reduced with age, implicating the clearance of micronuclei with aberrant DNA content. We found that micronucleus genetic content in the human brain preferentially contained content from larger chromosomes, consistent with prior reports of micronuclei in other genetically unstable systems such as the early post-fertilization zygote and in cancer[4,26,30]. Notably, chromosomes 13, 18, and 21 were consistent exceptions to the expected trend (Fig. S7d), which may reflect a general tolerance to aneuploidy in these three chromosomes in humans.

Reduction of large-scale CNA in the postnatal period

Comparison large-scale CNA patterns in neurons from individuals of different ages, revealed the proportion of cell carrying large-scale CNA decreases precipitously during the perinatal period (Fig. 4a) We evaluated potential confounders such as sample quality and number of cells per sample (Fig. S8), and concluded that the age of sample is the only significant factor associated with to the decrease in proportion of neurons with large-scale CNA after birth (logarithmic fit r^2=0.33, p=0.023). These results determined that prenatal cells have a clear difference in copy number distribution compared to postnatal samples.

In order to orthogonally define the cell types carrying large-scale CNA, we used multiomic single-nucleus ATAC/RNA (snATAC/RNA) sequencing to identify CNA using scATAC data concordantly with cell identity from scRNA data (Fig. S9). We generated snATAC/RNA libraries on three prenatal and two postnatal brains, and integrated this data with a prior published multiomic dataset from the human prefrontal cortex comprised of an additional prenatal and twelve postnatal brains[31]. We utilized the FOD metric to remove doublets[32], and then analyzed copy number variation from scATAC data using Epianeufinder[33]. Intriguingly, we identified a subpopulation of cells in the multiomic data that

appeared to be similar in CNA pattern to our large-scale CNA group ("large-scale CNA similar") (Fig. S9a-c). Similar to our results from scWGA, we observed a decline in the proportion of the "large-scale similar population" such that this population declines significantly in postnatal ages (Fig. S9d). The scRNA data from the multiome analysis showed that the "large-scale CNA similar" cluster was most prominent in mature excitatory and inhibitory neurons during neurodevelopment, although they were also present in progenitor and migrating cells (Fig. S9e), not surprisingly, as these are the precursors of mature neuronal types. In postnatal samples, the "large-scale CNA similar" cells were again predominantly neuronal, indicating that the genetic patterns observed represent a process most common to neurons (Fig. S9f).

Timescales of neuronal elimination differ by CNV scale and functional impact

We hypothesized that the observed selection against neurons with large-scale CNV likely has contributions from cell autonomous and non-cell autonomous effects. Non-cell autonomous effects are challenging to study in our postmortem frozen tissues, thus we focused on cell-autonomous impact and scale of affected genomic regions. We noted that selection appeared to occur in both the large-scale CNA population and among neurons with subchromosomal CNA observed in our "Diploid Predominant" signature cluster (CN1)(Fig. 5a-b). We then evaluated whether the scale of CNA affected the time course of selection. We found that after birth, while the large-scale CNA cluster had already reached a low plateau, suggesting that selection was complete, the proportion of cells with CNA in the Diploid Predominant cluster resulted in a significantly different trajectory ($p=0.05$), characterized by a slow decline over the course of a lifetime (Fig. 5b). Even amongst cells in the Diploid Predominant cluster, the size of CNA contributed to selection, as the size of altered regions was significantly smaller in postnatal compared to prenatal samples for copy losses ($p<.001$, Student t-test two-tailed). Thus, it appeared that larger-scale CNA, presumably involving larger numbers of genes, drove the rapid clearance occurring perinatally.

Given that neurons were preferentially affected by CNAs and by the process of removal of CNA-containing cells, we tested whether CNAs involving loss-of-function intolerant and critical neurodevelopmental genes were under-represented. We evaluated regions that showed more frequent copy loss in prenatal samples compared to postnatal samples, and assessed their relationship to known gene sets (Fig. 5d). We found that the significant regions of copy loss in prenatal neurons were depleted for loss-of-function intolerant genes, defined by high $pLI>0.9$ ($p<.032$, Fisher exact). Regions of copy loss in prenatal neurons were also depleted for genes associated with Autism spectrum Disorder (ASD), which are well characterized neurodevelopmental genes, defined by the SFARI Autism genes. ($p<.0028$, Fisher exact) may of which have effects in regulation neuronal development and plasticity (Fig. 5e). As a control, there was no depletion of genes with low pLI scores from regions of CNA. These results suggest that copy number loss of these specific neurodevelopmental genes drives at least in part the overall copy number landscape, even as aberrant genomes are generated.

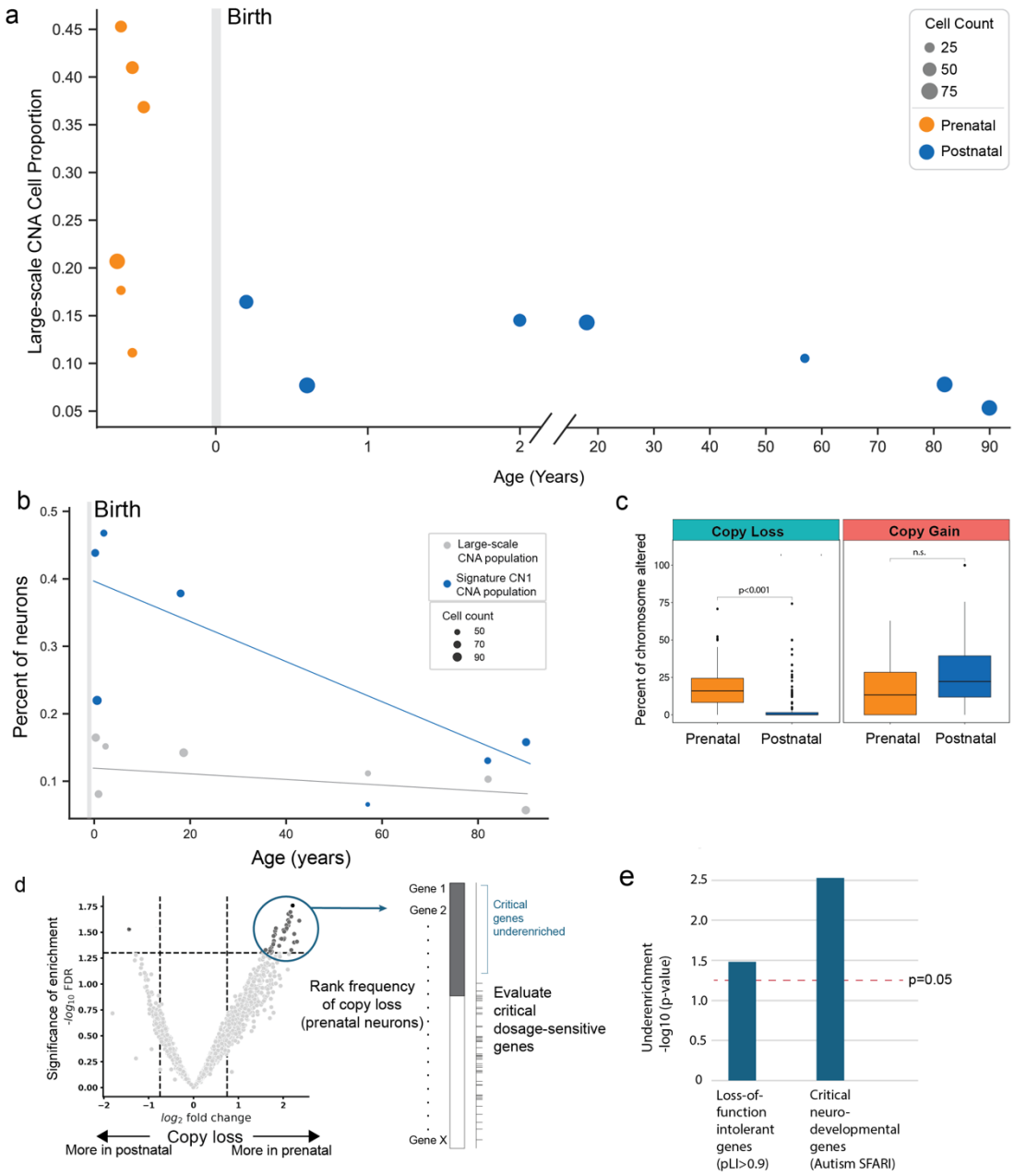

Figure 4. Selective elimination of neurons based on CNA size and involvement of dosage-sensitive genes.

a. Proportion of neurons with large-scale CNA over time, showing dramatic reduction in the perinatal period. Samples with fewer than 25 cells are omitted to ensure statistical robustness.
b. Differential timescale of elimination for neurons with large-scale CNA compared to neurons with subchromosomal CNA, observed in the Diploid Predominant CN1 signature cluster.

c. Total size of copy gains and losses (measured as percent of each chromosome altered) in the Diploid Predominant CN1 signature cluster.
d. Volcano plot showing the log scale FDR versus the log2 fold change of genes in copy loss regions between prenatal and postnatal neurons. Highlighted genes in the circled area represent those with significant enrichment, which are further evaluated for their functional relationship to specific gene categories.
e. Bar graph illustrating the underenrichment p-value of specific gene categories in regions of copy loss in prenatal samples, suggesting that loss of these gene categories may not be tolerated by the individual cell. The dashed line indicates a significance threshold at p = 0.05.

Together our results indicate a model (Fig. 5) whereby postmitotic prenatal neurons in the human cortical plate are genetically unstable, as witnessed by copy number signature profiles and biological markers of genetic instability. We describe a subpopulation of neurons with large-scale CNA, which are dramatically reduced in the perinatal period. Genetic selection acts early in neurodevelopment at the level of critical genes, and continues into the perinatal period depending on the scale of CNA and genes involved. Ultimately, these processes contribute to a further refined, increasingly genetically "normal" neuronal population over time.

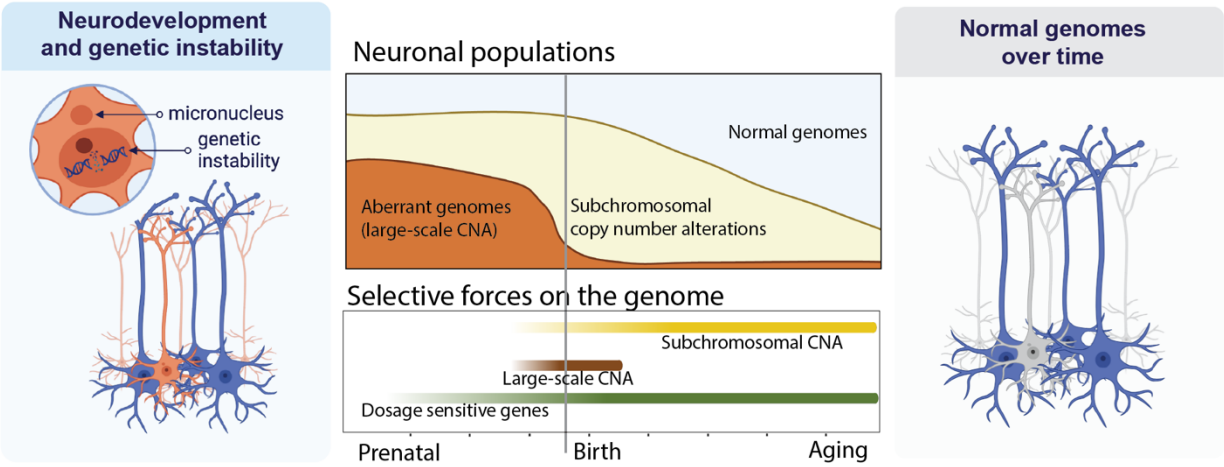

Figure 5. Schematic of findings from this study. Evidence for widespread genetic instability in postmitotic neurons during human neurodevelopment. Selective forces on the genome act on differential timescales, depending on scale of the CNA or gene functional impact, and shape the final genetic landscape of long-lived neurons.

Discussion

Our data suggest that widespread copy number variation is a prominent feature of early brain development, reminiscent of early post-fertilization zygotes, including genetic signatures of genetic instability and the formation of micronuclei[4,5,26]. Our observation that aberrant genomes characterized by large-scale CNA are more prevalent in neurons from the prenatal period than in postnatal neurons points to a developmental selection process acting perinatally that substantially re-shapes the final, surviving neuronal population.

Prior studies of neurons in the aging human cortex identified a trajectory of elimination similar to the one demonstrated by the subchromosomal CNAs identified in our "Diploid Predominant" Signature CN1 cluster[17]. Multiple studies in postnatal aged neurons refer to the large-scale CNAs that appear to persist in a subpopulation of neurons into old age[17,19]. Given the modest levels of aberrant genomes seen postnatally, our findings of widespread abnormalities in the prenatal brain was unexpected. We reviewed previously published single-cell sequencing data that described widespread aneuploidy in murine cortical neurons[11,34]. Visualization of these aneuploid murine neuronal genome profiles were reminiscent of the profiles seen in human prenatal neurons. Together these data suggest a mechanism of neuronal genetic variability and selection during neurodevelopment that likely is relevant across different species.

The observation that regions of copy loss are depleted for loss-of-function genes and neurodevelopmental disease genes suggests that selective mechanisms of genome quality control are linked to central nervous system development. In virtually all parts of the CNS that have been studied in detail, neurons are produced in greater numbers than survive into adulthood[35,36], with ongoing elimination during development, followed by a wave of cell elimination occurring after initial synaptic contacts are made, which in the case of human cerebral cortex occurs perinatally[21]. The mechanism of this neuronal elimination frequently involves competition among neurons for synaptic space, and neurons with CNA affecting synaptic proteins or regulators (such as the critical neurodevelopmental genes examined) would be expected to be at a competitive disadvantage in this process. This competition might provide a mechanism for selective removal of these CNA-containing neurons, re-framing this widely described process of "pruning" as a genome quality control method.

The reduction in CNAs observed after birth indicates an ongoing selection process that shapes the neuronal population with age, highlighting the role of genetic control in maintaining cognitive health. The perinatal period, up to a few years afterwards, may represent a critical window for determining the final set of neurons that persist into adulthood that is predominantly diploid. Further refinement of smaller subchromosomal CNAs then occurs throughout life, likely with some interplay to the functional importance of individual genes. Our findings open new avenues for investigating the mechanisms of genetic selection in the brain and their relevance to human disease.

References

1. Maury, E. A. *et al.* Enrichment of somatic mutations in schizophrenia brain targets prenatally active transcription factor bindings sites. *bioRxiv* 2022.02.23.481681 (2022) doi:10.1101/2022.02.23.481681.
2. Rodin, R. E. *et al.* The landscape of somatic mutation in cerebral cortex of autistic and neurotypical individuals revealed by ultra-deep whole-genome sequencing. *Nat. Neurosci.* **24**, 176–185 (2021).
3. McConnell, M. J. *et al.* Intersection of diverse neuronal genomes and neuropsychiatric disease: The Brain Somatic Mosaicism Network. *Science* **356**, (2017).
4. Currie, C. E. *et al.* The first mitotic division of human embryos is highly error prone. *Nat. Commun.* **13**, 6755 (2022).
5. Bolton, H. *et al.* Mouse model of chromosome mosaicism reveals lineage-specific depletion of aneuploid cells and normal developmental potential. *Nat. Commun.* **7**, 11165 (2016).
6. Starostik, M. R., Sosina, O. A. & McCoy, R. C. Single-cell analysis of human embryos reveals diverse patterns of aneuploidy and mosaicism. *Genome Res.* **30**, 814–825 (2020).
7. Palmerola, K. L. *et al.* Replication stress impairs chromosome segregation and preimplantation development in human embryos. *Cell* **185**, 2988-3007.e20 (2022).
8. van Echten-Arends, J. *et al.* Chromosomal mosaicism in human preimplantation embryos: a systematic review. *Hum. Reprod. Update* **17**, 620–627 (2011).
9. Vanneste, E. *et al.* Chromosome instability is common in human cleavage-stage embryos. *Nat. Med.* **15**, 577–583 (2009).
10. Sekar, S. *et al.* Complex mosaic structural variations in human fetal brains. *Genome Res.* **30**, 1695–1704 (2020).
11. Rehen, S. K. *et al.* Constitutional aneuploidy in the normal human brain. *J. Neurosci.* **25**, 2176–2180 (2005).

12. Abrahams, B. S. *et al.* SFARI Gene 2.0: a community-driven knowledgebase for the autism spectrum disorders (ASDs). *Mol. Autism* **4**, 36 (2013).

13. Karczewski, K. J. *et al.* The mutational constraint spectrum quantified from variation in 141,456 humans. *Nature* **581**, 434–443 (2020).

14. Shohat, S., Ben-David, E. & Shifman, S. Varying Intolerance of Gene Pathways to Mutational Classes Explain Genetic Convergence across Neuropsychiatric Disorders. *Cell Rep.* **18**, 2217–2227 (2017).

15. Spooren, W., Lindemann, L., Ghosh, A. & Santarelli, L. Synapse dysfunction in autism: a molecular medicine approach to drug discovery in neurodevelopmental disorders. *Trends Pharmacol. Sci.* **33**, 669–684 (2012).

16. Frankle, W. G., Lerma, J. & Laruelle, M. The synaptic hypothesis of schizophrenia. *Neuron* **39**, 205–216 (2003).

17. McConnell, M. J. *et al.* Mosaic copy number variation in human neurons. *Science* **342**, 632–637 (2013).

18. Chronister, W. D. *et al.* Neurons with Complex Karyotypes Are Rare in Aged Human Neocortex. *Cell Rep.* **26**, 825-835.e7 (2019).

19. Sun, C. *et al.* Mapping recurrent mosaic copy number variation in human neurons. *Nat. Commun.* **15**, 4220 (2024).

20. Yamaguchi, Y. & Miura, M. Programmed cell death in neurodevelopment. *Dev. Cell* **32**, 478–490 (2015).

21. Faust, T. E., Gunner, G. & Schafer, D. P. Mechanisms governing activity-dependent synaptic pruning in the developing mammalian CNS. *Nat. Rev. Neurosci.* **22**, 657–673 (2021).

22. Yamamoto, A. & Yue, Z. Autophagy and its normal and pathogenic states in the brain. *Annu. Rev. Neurosci.* **37**, 55–78 (2014).

23. Affymetrix. Median of the absolute values of all pairwise differences and quality control on Affymetrix genome-wide human SNP array 6.0. Preprint at https://assets.thermofisher.com/TFS-Assets/LSG/brochures/mapd_snp6_whitepaper.pdf (2008).

24. Zhao, Y. *et al.* High-resolution detection of copy number alterations in single cells with HiScanner. *bioRxiv* 2024.04.26.587806 (2024) doi:10.1101/2024.04.26.587806.

25. Adams, D. J. *et al.* Genetic determinants of micronucleus formation in vivo. *Nature* **627**, 130–136 (2024).

26. Klaasen, S. J. *et al.* Nuclear chromosome locations dictate segregation error frequencies. *Nature* **607**, 604–609 (2022).

27. Yano, S. *et al.* Propagation of neuronal micronuclei regulates microglial states. *bioRxiv* 2023.07.31.551211 (2023) doi:10.1101/2023.07.31.551211.

28. Steele, C. D. *et al.* Signatures of copy number alterations in human cancer. *Nature* **606**, 984–991 (2022).

29. Shimizu, N., Kanda, T. & Wahl, G. M. Selective capture of acentric fragments by micronuclei provides a rapid method for purifying extrachromosomally amplified DNA. *Nat. Genet.* **12**, 65–71 (1996).

30. Tovini, L. & McClelland, S. E. Impaired CENP-E Function Renders Large Chromosomes More Vulnerable to Congression Failure. *Biomolecules* **9**, (2019).

31. Herring, C. A. *et al.* Human prefrontal cortex gene regulatory dynamics from gestation to adulthood at single-cell resolution. *Cell* **185**, 4428-4447.e28 (2022).

32. Thibodeau, A. *et al.* AMULET: a novel read count-based method for effective multiplet detection from single nucleus ATAC-seq data. *Genome Biol.* **22**, 252 (2021).

33. Ramakrishnan, A. *et al.* epiAneufinder identifies copy number alterations from single-cell ATAC-seq data. *Nat. Commun.* **14**, 5846 (2023).

34. Rohrback, S. *et al.* Submegabase copy number variations arise during cerebral cortical neurogenesis as revealed by single-cell whole-genome sequencing. *Proc. Natl. Acad. Sci. U. S. A.* **115**, 10804–10809 (2018).

35. Kristiansen, M. & Ham, J. Programmed cell death during neuronal development: the sympathetic neuron model. *Cell Death Differ.* **21**, 1025–1035 (2014).

36. Becker, E. B. E. & Bonni, A. Cell cycle regulation of neuronal apoptosis in development and disease. *Prog. Neurobiol.* **72**, 1–25 (2004).

Acknowledgements

We acknowledge the sacrifices of the donors who provided tissue for this study to advance our understanding of the brain. Tissue sources were provided by the University of Maryland Brain and Tissue Bank. We acknowledge the Boston Children's Hospital Flow Cytometry Core for developing and carrying out protocols to isolate single neurons. We acknowledge David S. Pellman and Greg Brunette for thoughtful discussion about identifying evidence for genetic instability. We acknowledge Peter Ly for sharing of micronuclei isolation protocols and helpful discussion. We acknowledge Takeshi Nagata for supporting micronuclear analysis.

Funding:

D.D.S. is supported by National Institutes of Health (NIH) National Institutes of Neurological Disorders and Stroke (NINDS) K08-NS128074. D.D.S., U.G., and C.A.W are supported by the Templeton Foundation. C.A.W is supported by the Howard Hughes Medical Institute (HHMI), NINDS R01NS032457, NIA R01AG070921, UG3NS132138, and 1UG3NS132144. Y.Z., J.B., and P.J.P are supported by R01-HG012573 and R01-CA269805. S.Z. is supported by the Program in Genetics and Genomics PhD Training Grant T32GM141745.

Author Contributions:

D.D.S, Y.Z., P.J.P, C.A.W conceptualized, supervised, and designed this project. C.A.W., and P.J.P. provided resources for this project. D.D.S., J.B., J.T., T.T., F.T., and Y.Z. performed analysis. U.G., S.Z., X.Q., and D.D.S. performed experiments. D.D.S., Y.Z., and U.G. wrote the manuscript. All authors provided edits to the manuscript.

Competing Interests:

P.J.P. is a member of the scientific advisory board for Bioskryb Genomics, Inc.

Data and materials availability:

Sample transfer is restricted by material transfer agreement. Data will be deposited on dbGap. Code will be made available on GitHub:

Supplementary Materials

Figs. S1 to S9.

Tables S1 to S3.

Materials and Methods